Examining the Relative Timing of Hydrogen Abstraction Steps during NAD^+-Dependent Oxidation of Secondary Alcohols Catalyzed by Long-Chain D-Mannitol Dehydrogenase from *Pseudomonas fluorescens* Using pH and Kinetic Isotope Effects†

Mario Klimacek and Bernd Nidetzky*

Division of Biochemical Engineering, Institute of Food Technology, University of Agricultural Sciences Vienna, Muthgasse 18, A-1190 Vienna, Austria, and Institute of Biotechnology, Technical University of Graz, Petersgasse 12/I, A-8010 Graz, Austria

Received January 7, 2002; Revised Manuscript Received April 18, 2002

ABSTRACT: Mannitol dehydrogenases (MDH) are a family of Zn^{2+}-independent long-chain alcohol dehydrogenases that catalyze the regiospecific NAD^+-dependent oxidation of a secondary alcohol group in polyol substrates. pH and primary deuterium kinetic isotope effects on kinetic parameters for reaction of recombinant MDH from *Pseudomonas fluorescens* with D-mannitol have been measured in H_2O and D_2O at 25 °C and used to determine the relative timing of C−H and O−H bond cleavage steps during alcohol conversion. The enzymatic rates decreased at low pH; apparent pK values for $\log(k_{cat}/K_{mannitol})$ and $\log k_{cat}$ were 9.2 and 7.7 in H_2O, respectively, and both were shifted by +0.4 pH units in D_2O. Proton inventory plots for k_{cat} and $k_{cat}/K_{mannitol}$ were determined at pL 10.0 using protio or deuterio alcohol and were linear at the 95% confidence level. They revealed the independence of primary deuterium isotope effects on the atom fraction of deuterium in a mixed H_2O-D_2O solvent and yielded single-site transition-state fractionation factors of 0.43 ± 0.05 and 0.47 ± 0.01 for $k_{cat}/K_{mannitol}$ and k_{cat}, respectively. $^D(k_{cat}/K_{mannitol})$ was constant (1.80 ± 0.20) in the pH range 6.0−9.5 and decreased at high pH to a limiting value of ≈1. Measurement of $^D(k_{cat}/K_{fructose})$ at pH 10.0 and 10.5 using NADH deuterium-labeled in the 4-pro-*S* position gave a value of 0.83, the equilibrium isotope effect on carbonyl group reduction. A mechanism of D-mannitol oxidation by MDH is supported by the data in which the partly rate-limiting transition state of hydride transfer is stabilized by a single solvation catalytic proton bridge. The chemical reaction involves a pH-dependent internal equilibrium which takes place prior to C−H bond cleavage and in which proton transfer from the reactive OH to the enzyme catalytic base may occur. Loss of a proton from the enzyme at high pH irreversibly locks the ternary complex with either alcohol or alkoxide bound in a conformation committed of undergoing NAD^+ reduction at a rate about 2.3-fold slower than the corresponding reaction rate of the protonated complex. Transient kinetic studies for D-mannitol oxidation at pH(D) 10.0 showed that the solvent isotope effect on steady-state turnover originates from a net rate constant of NADH release that is ≈85% rate-limiting for k_{cat} and 2-fold smaller in D_2O than in H_2O.

The regiospecific $NAD(P)^+$-dependent oxidation of polyalcohols by secondary alcohol dehydrogenases (secADHs)[1] has attracted much interest because it is of great importance in all forms of metabolism and has numerous practical applications in chiral synthesis (*1*, *2*). In a widely used classification based on similarities at the primary structure level, secADHs fall into the short-, medium-, and long-chain ADH families (*3*−*5*). Structure−function relationships for short-chain and medium-chain ADHs have been well-established (*6*−*9*). However, little is known about the long-chain counterpart enzymes (*10*). Mechanistically, medium-chain ADHs are special among ADHs in regard to their utilization of electrophilic Zn^{2+} in catalysis (*11*). As no significant sequence similarities prevail across the ADH families, the study of long-chain ADHs is interesting in order to complete the picture of $NAD(P)^+$-dependent ADH mechanisms in terms of both structure and enzymic redox chemistry.

Mannitol 2-dehydrogenase from *Pseudomonas fluorescens* (PsMDH), a member of the mannitol dehydrogenase (MDH) family of enzymes (*12*, *13*), is a representative Zn^{2+}-independent long-chain ADH (*14*). It is a monomeric 54-kDa enzyme and catalyzes the NAD^+-dependent oxidation of D-mannitol in physiology, as shown in eq 1

$$\text{D-mannitol} + NAD^+ \leftrightarrow \text{D-fructose} + NADH + H^+ \quad (1)$$

† Supported by the Austrian Science Funds, Grants P-12569-MOB and P-15208 to B.N.

* Corresponding author address: Dr. Bernd Nidetzky, Institute of Biotechnology, Petersgasse 12/I, A-8010 Graz, Austria. Phone: (+43)-316-873-8400. Fax: (+43)-316-873-8434. E-mail: bernd.nidetzky@tugraz.at.

[1] Abbreviations: ADH, alcohol dehydrogenase; secADH, secondary ADH; KIE, primary kinetic isotope effect; S-KIE, solvent kinetic isotope effect; MDH, mannitol dehydrogenase; PsMDH, recombinant MDH from *Pseudomonas fluorescens*; FDH, formate dehydrogenase; NADD, (4*S*)-[4-^2H]-NADH; formate-*d*, [^2H]-CO_2^-; D-mannitol-*d*, 2-[^2H]-D-mannitol.

10.1021/bi025517x CCC: $22.00
Published on Web 07/09/2002

PsMDH is specific for transferring the pro-4-*S* hydrogen of NADH and utilizes a steady-state ordered bi-bi kinetic mechanism in which coenzyme binds first and leaves last (*14*). pH and isotope effect studies for the direction of D-fructose reduction by PsMDH have suggested a stepwise enzymic mechanism in which the pH-sensitive and isotope-dependent steps are different (*14*). Medium-chain ADH provides a canonical mechanism of stepwise dehydrogenase reaction in which a zinc-bound alkoxide is a central intermediate (*11*, *15*, *17*−*21*). In the direction of alcohol oxidation, zinc ion facilitates proton removal from the reactive OH group by stabilizing the alkoxide, which should undergo faster hydrogen transfer than would the zinc-bound alcohol. In reverse reaction, the C═O bond is polarized by electrophilic interactions with Zn^{2+}, which should increase the extent of C^+-O^- charge separation and reduce the energy barrier for C−H bond formation (*21*).

The present paper reports results of pH and isotope effect studies that were designed to determine the relative timing of hydrogen abstraction steps during alcohol/carbonyl interconversion catalyzed by PsMDH. The problem was considered significant because a basic unanswered question of ADH mechanisms pertains to differences in the catalytic reaction profiles of medium-chain ADH and other zinc-independent ADHs. The data and their interpretation provide clear evidence for a mechanism of PsMDH in which there is a pH-dependent internal equilibrium involving the D-mannitol-bound enzyme prior to C−H bond cleavage. The removal of the hydroxyl proton and formation of an alkoxide intermediate may occur in this pre-equilibrium. A single solvation catalytic proton bridge stabilizes the rate-limiting transition state of hydride transfer, and this could indicate a proton relay mechanism.

MATERIALS AND METHODS

Materials. If not mentioned otherwise, all chemicals were of the highest purity available from Sigma (St. Louis, MO). NAD^+ and NADH were from Seppim (France) and were 99.5% pure. (4*S*)-[4-^{2}*H*]NADH (NADD) with an isotopic purity of ≥98% was prepared enzymatically (*22*). Deuteriumoxid containing 99.8% deuterium was from Chemotrade GesmbH (Leipzig, Germany).

Enzymes. Recombinant PsMDH carrying a C-terminal metal-affinity fusion (*13*) was prepared as described recently (*14*). Formate dehydrogenase (FDH) from *Candida boidinii* was from ASA Spezialenzyme GmbH (Braunschweig, Germany) and was used after purification by gel filtration (Sephadex G-25 material; PD-10 column; Amersham Pharmacia Biotech, Cleveland, OH) to remove glycerol present in the commercial preparation. The enzyme activities of MDH and FDH were measured at pH 10 and 7.0, respectively, using spectrophotometric assays in which the rate of formation of NADH was recorded from the time-dependent increase in absorbance at 340 nm ($\epsilon_{NADH} = 6220\ M^{-1}\ cm^{-1}$). The MDH activity was determined in 50 mM glycine/NaOH buffer using 20 mM D-mannitol and 3 mM NAD^+. The FDH activity was determined in 50 mM sodium phosphate buffer using 500 mM sodium formate and 3 mM NAD^+. One unit of enzyme activity refers to 1 μmol of NADH formed per minute under the conditions used. The molar concentrations of PsMDH solutions were determined by using a value of 54 000 $M^{-1}cm^{-1}$ for the molar extinction coefficient of the enzyme at 280 nm, as deduced from the amino acid sequence of PsMDH (*13*).

2-[^{2}H]-D-Mannitol. We used an enzymatic procedure for the synthesis of 2-[^{2}*H*]-D-mannitol (D-mannitol-*d*) according to eq 2

$$\text{D-fructose} + [^2H]\text{-}CO_2^- + H^+ \leftrightarrow 2\text{-}[^2H]\text{-D-mannitol} + CO_2 \quad (2)$$

The reaction was carried out at 25 °C in 100 mM Tris/HCl buffer, pH 7.5, containing 0.5 mM DTT to stabilize the enzymes. A solution (≈100 mL) of sodium formate-*d* (300 mM), D-fructose (300 mM), and NAD^+ (0.5 mM) was incubated in the presence of PsMDH (5 U/mL) and FDH (1 U/mL), typically for 24 h, until the conversion of the substrates was greater than 90%. Protein was then removed by ultrafiltration in an Amicon stirred cell equipped with a 30-kDa cutoff YM membrane. The ultrafiltration permeate was desalted with Lewatit S100 and Lewatit S4428. D-Mannitol-*d* was crystallized from the aqueous solution. The product comigrated and coeluted with authentic D-mannitol in TLC and HPLC, respectively, and was estimated to be ≥95% pure. Deuteration at C-2 of D-mannitol-*d* was proven by ^{1}H and ^{13}C NMR spectroscopy, and the isotopic purity of the compound was estimated to be greater than 98%.

Kinetic Studies at the Steady State. Initial rates of D-mannitol oxidation and D-fructose reduction were measured at 25 ± 0.5 °C with a Beckman DU-650 spectrophotometer by recording the increase and decrease in the absorbance of NADH at 340 nm, respectively. If not mentioned otherwise, all initial-rate data were acquired under conditions in which the substrate (or the coenzyme) was varied at a constant and saturating concentration of the coenzyme (or the substrate).

pH studies were carried out for the direction of NAD^+-dependent oxidation of D-mannitol using D-mannitol or D-mannitol-*d* as the varied substrate. Experiments were performed in H_2O and D_2O using 50 mM MES/NaOH buffer (pL 5.5−7.0), 50 mM Tris/HCl buffer (pL 7.0−9.0), or 50 mM glycine/NaOH buffer (pL 9.0−11.0). Overlapping pH ranges were chosen to ensure detection of possible inhibition of PsMDH by buffer components.

Primary deuterium kinetic isotope effects (KIE) on apparent kinetic parameters for oxidation of D-mannitol and reduction of D-fructose were obtained from initial-rate measurements with D-mannitol-*d* and NADD, respectively, and by directly comparing results with the unlabeled and deuterium-labeled substrate (or coenzyme). Solvent deuterium isotope effects (S-KIEs) were obtained at identical pL values of 10.0 in H_2O and D_2O. The pD of buffers made with D_2O was corrected for the isotope effect on the response of the pH electrode according to pD = meter reading +0.4 (*23*).

Proton inventory studies were performed at pL 10.0 using a 50 mM glycine buffer containing a varying atom fraction (*n*) of deuterium in the solvent. The mixed isotopic solution was prepared from glycine buffers, pL 10.0, made with H_2O and D_2O, and the actual pL values of these solution were uncorrected. Stock solutions of D-mannitol and D-mannitol-*d* (10 mM each) were prepared in the respective buffers. Initial rates were recorded for varied substrate concentrations at

10 different values of *n*, and KIEs and S-KIEs were obtained from these data.

Rapid Mixing Experiments. Fast kinetic studies of PsMDH-catalyzed oxidation of D-mannitol were carried out at 25 °C in 50 mM glycine/NaOH(D) buffer, pL 10.0, with an Applied Photophysics stopped-flow reaction analyzer (model SX.18 MV). Under the conditions used, the instrument had a dead time of approximately 1.5 ms. Data acquisition and analysis were done with Applied Photophysics software. All experiments were performed in triplicate, and the resulting stopped-flow traces were averaged and then used for further analyses. The enzyme solution contained coenzyme to generate the enzyme−nucleotide complex before the reaction was started by mixing the enzyme and substrate solutions. Transient kinetic measurements were carried out in H_2O and D_2O under conditions where [E] was varied and limiting, thus allowing multiple turnovers of the enzyme present.

Data Processing. Figures show the experimentally determined values, and curves are calculated from nonlinear fits of the data to the appropriate equation using the least-squares method with the program SigmaPlot 2000 (SPSS). Linear double reciprocal plots were fitted to eq 3 where v is the initial rate, k_{cat} is the turnover number, and K_A is a Michaelis constant. [E] and [A] are molar concentrations of the enzyme and a substrate. Equation 4 describes an intersecting initial rate pattern for a two substrate reaction where K_{iA} is the dissociation constant of the substrate binding first. Equation 5 was used when linear competitive inhibition was observed, and [I] is the molar inhibitor concentration. Equation 6a was used to determine KIEs and S-KIEs on kinetic parameters where F_i is the fraction of deuterium in the substrate or in the solvent and $E_{V/K}$ and E_V are the isotope effects minus 1 on k_{cat}/K and k_{cat}. An S-KIE on an inhibitor-binding constant (K_{is}) was determined by using eq 6b where E_{Ki} is the isotope effect minus 1 on K_{is}. pH profiles were fitted to either eqs 7a, b, or c. Equation 7a describes log Y vs pH curves that are level above pK_1 but decrease with slope of +1 below pK_1. Equation 7b is the mirror image of eq 7a where a decrease of log Y occurs with −1 slope above pK_1. Equation 7c describes a wave with constant values at high (C_H) and low pH (C_L). In eqs 7a and b, C is the pH-independent value of Y at the optimal state of protonation. Proton inventory data were fitted to eq 8 where Φ^{TS} is the transition state (TS) fractionation factor. ^nk is the differential isotope effect on k (H_2O vs mixed isotopic solvent with deuterium content n), and ^{D_2O}k is the full isotope effect on k (H_2O vs D_2O). Equation 9 describes "burst" kinetics in which an exponential increase in absorbance (A_t) is followed by a linear steady-state increase in A_t. Π is the burst constant; k_{trans} (s^{-1}) and k_{ss} ($\Delta A_t\ s^{-1}$) are rate constants.

$$v = k_{cat}[E][A]/(K_A + [A]) \quad (3)$$

$$v = k_{cat}[E][A][B]/(K_{ia}K_B + K_A[B] + K_B[A] + [A][B]) \quad (4)$$

$$v = k_{cat}[E][A]/(K_A(1 + [I]/K_{is}) + [A]) \quad (5)$$

$$v = k_{cat}[E][A]/(K_A(1 + F_iE_{V/K}) + [A](1 + F_iE_V)) \quad (6a)$$

$$v = k_{cat}[E][A]/(K_A(1 + [I]/K_{is}(1 + F_iE_{Ki})) + [A]) \quad (6b)$$

$$\log Y = \log [C/(1 + [H^+]/K_1)] \quad (7a)$$

$$\log Y = \log [C/(1 + K_1/[H^+])] \quad (7b)$$

$$\log Y = \log [(C_L + C_HK_1/[H^+])/(1 + K_1/[H^+])] \quad (7c)$$

$$^nk = {}^{D_2O}k(1 - n + n\Phi^{TS}) \quad (8)$$

$$A_t = \Pi(1 - e^{-k_{trans}t}) + k_{ss}t \quad (9)$$

Table 1: Kinetic Parameters of MDH at pH 10.0.[a]

k_{cato} (s^{-1})	40 ± 0.5
$K_{mannitol}$ (mM)	0.40 ± 0.02
$k_{cat}/K_{mannitol}$ ($M^{-1}\ s^{-1}$)	1.0×10^5
K_{NAD^+} (μM)	93 ± 8
k_{cat}/K_{NAD^+} ($M^{-1}\ s^{-1}$)	4.0×10^5
K_{iNAD^+} (μM)	300 ± 50
k_{catr} (s^{-1})	20 ± 0.7
$K_{fructose}$ (mM)[b]	0.44 ± 0.05
$k_{cat}/K_{fructose}$ ($M^{-1}\ s^{-1}$)[b]	4.5×10^4
K_{NADH} (μM)	10 ± 2
k_{cat}/K_{NADH} ($M^{-1}\ s^{-1}$)	2.0×10^6
K_{iNADH} (μM)	30 ± 7
	100 ± 30[c]
K_{eq} (M)	2.2×10^{-9}[d]
	2.0×10^{-9}[e]

[a] Kinetic parameters were obtained from nonlinear fits to eq 4, using initial velocities determined in the direction of D-mannitol oxidation (o) and fructose reduction (r) at pH 10.0. [b] Based on 1% free carbonyl form in aqueous solution. [c] Obtained from a linear competitive inhibition of NADH versus NAD^+ and fits of data to eq 5. [d] Thermodynamic equilibrium constant, calculated by using the Haldane relationship for an ordered bi-bi kinetic mechanism and correction for the pH dependence of the observed equilibrium constant (appK_{eq}) according to $K_{eq} = \text{app}K_{eq}[H^+]$. [e] Experimental value of K_{eq} determined according to eq 1 and using an average value from five independent experimental determinations.

RESULTS

Steady-State Kinetic Parameters of PsMDH at pH 10.0. Initial rates of NAD^+-dependent oxidation of D-mannitol and NADH-dependent reduction of D-fructose were recorded in the absence of products at pH 10.0 and 25 °C. In each direction of the reaction (eq 1), they were acquired under conditions where the substrate was varied at several constant levels of the coenzyme. The experimental data were fitted to eq 4 and results are summarized in Table 1. The internal consistency of the kinetic parameters was verified by thermodynamic analysis, using the Haldane relationship for an ordered bi-bi mechanism.

pL Profiles of Kinetic Parameters in H_2O and D_2O. Initial velocities of NAD^+-dependent oxidation of D-mannitol were measured at constant saturating NAD^+ levels (3 mM) with D-mannitol as the varied substrate in H_2O or D_2O in the pL range 5.5−11.0. Equation 3 was used to fit the initial-rate data acquired at each pL value, and the pL dependences of k_{cat} and $k_{cat}/K_{mannitol}$ are shown in Figures 1 and 2, respectively. Kinetic parameters for PsMDH were level at high pL and decreased with +1 slope below their optimum pL values. The pL profiles in Figures 1 and 2 were fitted to eq 7a, and resulting pK values are shown in Table 2.

pH Profiles of KIEs. Values of $^Dk_{cat}$ and $^D(k_{cat}/K_{mannitol})$[2] were obtained at several different pH values in the pH range

[2] The nomenclature of Northrop (*24*) is used, whereby $^Dk_{cat}$ and $^D(k_{cat}/K)$ are primary deuterium KIEs on k_{cat} and k_{cat}/K, respectively, and $^{D_2O}k_{cat}$ and $^{D_2O}(k_{cat}/K)$ are solvent deuterium KIEs on the same kinetic parameters.

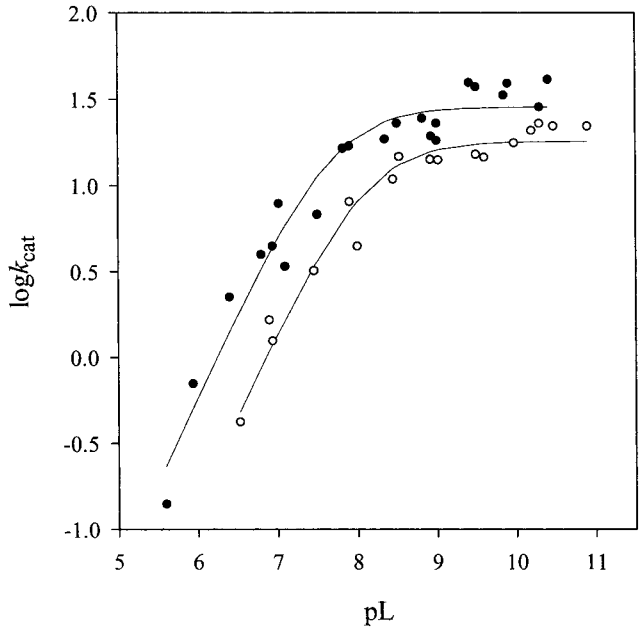

FIGURE 1: pL profiles of log k_{cat} for D-mannitol oxidation measured in H_2O (full circles) and D_2O (open circles). Initial velocities were recorded at different pL values with D-mannitol as the varied substrate, using constant saturating concentrations of NAD^+ (3 mM). k_{cat} values at each pL were obtained from fits of the data to eq 3. The lines show the fits of log k_{cat} data to eq 7a.

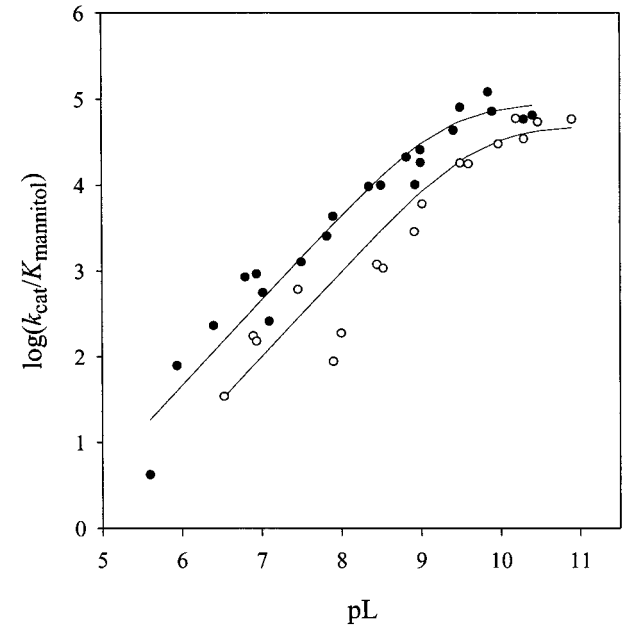

FIGURE 2: pL dependence of log($k_{cat}/K_{mannitol}$) determined in H_2O (full circles) and D_2O (open circles). The conditions used were as in Figure 1. The lines show the fits of log($k_{cat}/K_{mannitol}$) data to eq 7a.

6.0−10.5 by direct comparison of initial-rate data measured with either D-mannitol or D-mannitol-*d* as the varied substrate and constant, saturating NAD^+ (3 mM). Equation 6a was used to fit the data recorded at each pH. The pH profiles of KIEs on k_{cat} and $k_{cat}/K_{mannitol}$ are shown in Figure 3. $^Dk_{cat}$ went through a wave (eq 7c) and had constant values of 1.07 and 1.21 at high and low pH, respectively. $^D(k_{cat}/K_{mannitol})$ had a constant value of 1.8 in the pH range 6.0−9.5 and decreased to a value of ≈1 above an apparent p*K* of ≈10.9 (eq 7b). At pH 6.5 where the pH profiles of both k_{cat} and $k_{cat}/K_{mannitol}$ decreased with +1 slope (Figures 1 and 2), $^Dk_{cat}$ and $^D(k_{cat}/K_{mannitol})$ reached limiting, however, different values.

Table 2: p*K* Values from pL Profiles of the Kinetic Parameters and Isotope Effects

parameter	pK_1	*C*
$\log(k_{cato})_{H_2O}$[a]	7.7 ± 0.1	29 ± 3 (s^{-1})
$\log(k_{cat}/K_{mannitol})_{H_2O}$[a]	9.2 ± 0.3	9. 10^4 ± 2. 10^4 (M^{-1} s^{-1})
$\log(k_{cato})_{D_2O}$[a]	8.1 ± 0.1	18 ± 1 (s^{-1})
$\log(k_{cat}/K_{mannitol})_{D_2O}$[a]	9.7 ± 0.5	5. 10^4 ± 2. 10^4 (M^{-1} s^{-1})
log $^Dk_{cato}$[b,d]	7.6 ± 0.7	C_H = 1.07 ± 0.02 C_L = 1.21 ± 0.04
log $^D(k_{cat}/K_{mannitol})$[c,d]	10.9 ± 0.9	1.8 ± 0.1

[a] eq 7a was used to fit the pL dependences of log k_{cato} and log($k_{cat}/K_{mannitol}$) in H_2O and in D_2O. The correlation coefficients given in the nonlinear regression reports by the SigmaPlot 2000 program were 0.92 or greater, indicating a good fit of the data despite some experimental scatter obvious in Figures 1 and 2. Note that the parameter standard deviation is a calculated one and does not reflect the result of several independent determinations. [b,c] The pH dependences of log $^Dk_{cat0}$ and log $^D(k_{cat}/K_{mannitol})$ were fitted to eqs 7c and 7b, respectively. [d] Correlation coefficients were smaller than 0.88, reflecting variation in experimental determination of KIEs and resulting in relatively large standard errors for estimated p*K* values.

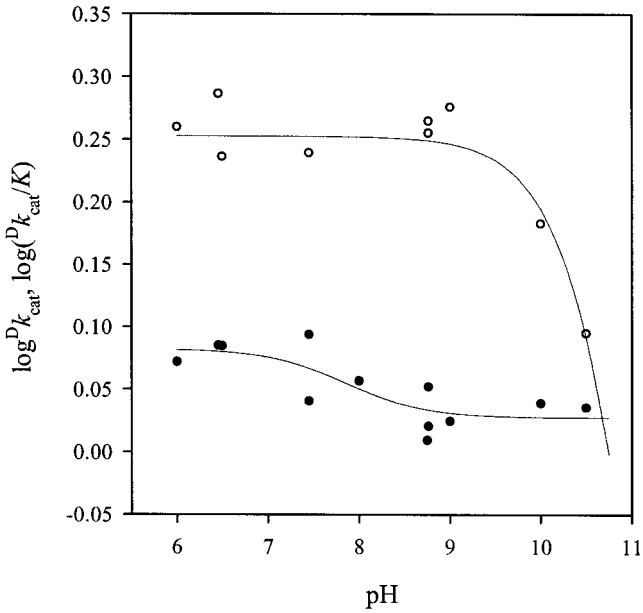

FIGURE 3: pH dependence of the primary deuterium isotope effect in the direction of D-mannitol oxidation. $^Dk_{cat}$ (full circles) and $^D(k_{cat}/K_{mannitol})$ (open circles) values were determined from fits to eq 6a of initial rates measured with varied concentrations of D-mannitol and D-mannitol-*d* using saturating levels of NAD^+ (3 mM). The lines show nonlinear fits of the $^D(k_{cat}/K_{mannitol})$ and $^Dk_{cat}$ data to eqs 7b and 7c, respectively.

Primary Deuterium Isotope Effects. KIEs on kinetic parameters for the forward and reverse directions of the PsMDH-catalyzed reaction were measured in H_2O and D_2O at pL 10.0 and are summarized in Table 3. $^Dk_{cat}$, $^D(k_{cat}/K_{substrate})$, and $^D(k_{cat}/K_{coenzyme})$ showed little dependence on the solvent H_2O or D_2O. $^D(k_{cat}/K_{fructose})$ at pL 10.0 was an exception because the KIE in water was inverse,[3] whereas a significant normal isotope effect was observed in D_2O.

Solvent Isotope Effects. The S-KIEs on kinetic parameters for D-mannitol oxidation and on binding constants for NADH and NAD^+ were measured at pL 10.0 in H_2O and in D_2O. Because the pH profiles for k_{cat}, $k_{cat}/K_{mannitol}$ (Figures 1 and 2), and K_{iNADH} (determined in ref *14*) approach plateau values

Table 3: Primary Deuterium Kinetic Isotope Effects on MDH Catalysis in H_2O and D_2O at pL 10.0[a]

parameter	H_2O	D_2O
$^{D}k_{cato}$	1.10 ± 0.04	1.07 ± 0.03
$^{D}(k_{cat}/K_{mannitol})$	1.80 ± 0.20	1.69 ± 0.10
$^{D}(k_{cat}/K_{NAD^+})$	0.94 ± 0.13	0.99 ± 0.10
$^{D}k_{catr}$	0.90 ± 0.07	0.98 ± 0.05
$^{D}(k_{cat}/K_{fructose})$	0.83 ± 0.15	1.80 ± 0.20
$^{D}(k_{cat}/K_{NADH})$	1.12 ± 0.22	0.81 ± 0.07

[a] Parameters were calculated from fits to eq 6a, using initial rate data determined at 25 °C in 50 mM glycine/NaOH(D) buffer, pL 10.0.

Table 4: Solvent Isotope Effects on MDH Catalysis at pL 10.0[a]

parameter	
$^{D_2O}k_{cato}$	1.73 ± 0.10
$^{D_2O}(k_{cat}/K_{mannitol})$	2.36 ± 0.30
$^{D_2O}(k_{cat}/K_{NAD^+})$	1.16 ± 0.18
$^{D_2O}K_{iNADH}$[b]	2.00 ± 0.60
$^{D_2O}K_{iNAD^+}$[b]	0.99 ± 0.25

[a] Parameters were calculated from fits to eq 6a, using initial rate data determined at 25 °C in H_2O and in D_2O with a 50 mM glycine/NaOH(D) buffer, pL 10.0. [b] Solvent isotope effects on K_i values for coenzymes were determined from competitive inhibitor binding studies and nonlinear fits of eq 6b to the data.

at the pH of measurement, an observed sizable S-KIE is real and does not reflect a difference in the pL profiles of the respective parameter in H_2O and D_2O. Values for $^{D_2O}k_{cat}$ and $^{D_2O}(k_{cat}/K)$ are summarized in Table 4. $^{D_2O}k_{cat}$ and $^{D_2O}(k_{cat}/K_{mannitol})$ were both greater than 1, indicating a medium effect or a contribution of proton-transfer reactions to rate limitation for k_{cat} and $k_{cat}/K_{mannitol}$. By contrast, the significance of $^{D_2O}(k_{cat}/K_{NAD^+})$ being different from 1 was not clear on the 80% probability level. Inhibition patterns of NAD^+ and NADH were determined at 400 mM D-fructose and 50 mM D-mannitol, and a fit of eq 6b to the data gave K_{iNAD^+} or K_{iNADH} and the S-KIE on the respective binding constant (Table 4). No S-KIE on K_{iNAD^+} was observed, whereas the value of $^{D_2O}K_{iNADH}$ was greater than 1.

Proton Inventory Studies. Kinetic parameters k_{cat} and $k_{cat}/K_{mannitol}$ were determined at pL 10.0 with either D-mannitol or D-mannitol-*d* as the varied substrate in binary mixtures of H_2O and D_2O containing a varying atom fraction of deuterium in the solvent. As shown in Figure 4, parts a and b, the proton inventories for k_{cat} and $k_{cat}/K_{mannitol}$ appeared to be linear, and the values of $^{D}k_{cat}$ and $^{D}(k_{cat}/K_{mannitol})$ were independent of the degree of solvent deuteration. Least-squares regression analysis for the k_{cat} and $k_{cat}/K_{mannitol}$ proton inventories using eq 8 gave correlation coefficients (r^2) of 0.996 and 0.986 with high F values of 1740 and 174 at a significance level of $P < 0.0001$, respectively. Therefore, these results *support* a single-proton-bridge model for both kinetic parameters, although they, clearly, cannot prove it. The precision level that is required of proton inventory data to discriminate among linear and higher-order models (tabulated in ref *23*) was achieved with k_{cat} values (±1.6%).

[3] A value of <0.90 for $^{D}(k_{cat}/K_{fructose})$ at pH 10.0 has been confirmed in four independent determinations of the isotope effect. The standard deviations for the KIE estimates obtained from a nonlinear fit of eq 6a to initial-rate data recorded with NADH and NADD were typically in the range 0.10−0.15. They, probably, reflect a limit to the statistical accuracy of the KIE under the conditions used. However, a KIE value of <0.90 appears to be well-supported by the data.

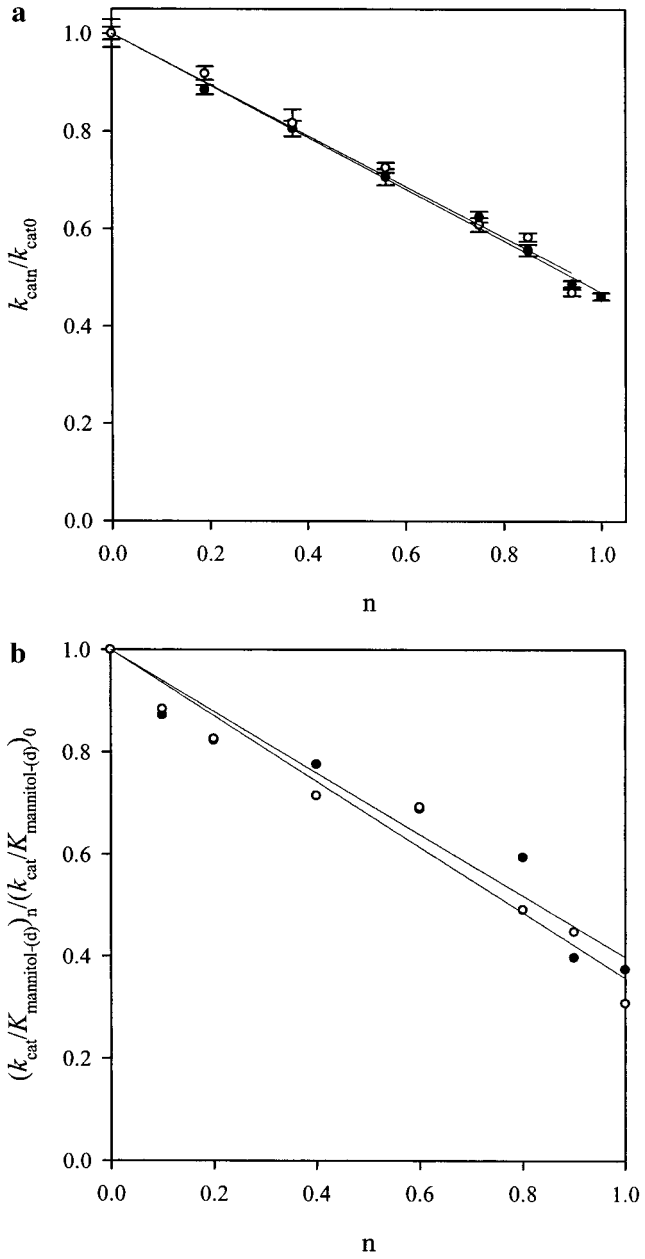

FIGURE 4: Proton inventory plots for k_{cat} (panel a) and $k_{cat}/K_{mannitol}$ (panel b) using either D-mannitol (full circles) or D-mannitol-*d* (open circles) as the substrate. Kinetic parameters were obtained from initial rate measurements in mixed isotopic solvents of H_2O and D_2O containing a varying atom fraction (n) of deuterium. The reactions were carried out at 25 °C in 50 mM glycine buffer, pL 10.0. Results are shown as ratios using kinetic parameters in H_2O (k_{cat0}; $(k_{cat}/K_{mannitol})_0$) as reference values. Lines are linear fits of the data using eq 8. Error bars show the standard errors for k_{cat} in panel a. The standard error for $k_{cat}/K_{mannitol}$ values was approximately ±6%.

The precision of ±6% for $k_{cat}/K_{mannitol}$ values is above the theoretical level of ±2.8% (*23*). However, the one-proton model is the simplest model that agrees satisfactorily with the proton inventory data for $k_{cat}/K_{mannitol}$. The fit of the data to eq 8 yielded transition-state fractionation factors of 0.47 ± 0.01 and 0.43 ± 0.05 for k_{cat} and $k_{cat}/K_{mannitol}$, respectively.

Pre-Steady-State Kinetic Studies with Multiple Turnover of the Enzyme. Stopped-flow kinetic experiments for PsMDH-catalyzed oxidation of D-mannitol were carried out at pL 10.0 using varied concentrations of PsMDH in the range 2−15 μM and constant levels of NAD^+ (0.2 mM) and D-mannitol

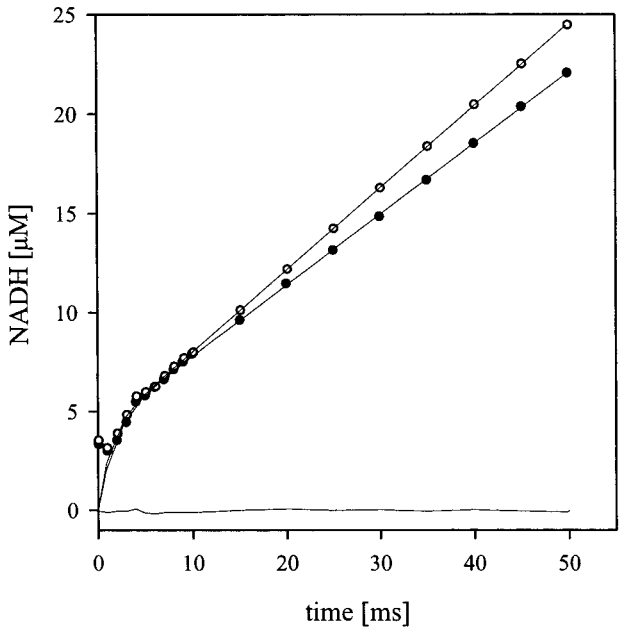

FIGURE 5: Typical stopped-flow progress curves obtained under conditions of limiting enzyme concentration. Reactions were carried out in 50 mM glycine/NaOH(D) buffer, pH 10.0 (open circles) or pD 10.0 (full circles) using 14 μM PSMDH, 10 mM D-mannitol, and 200 μM NAD^+. The lines show the fit of eq 9 to the experimental absorbance traces. The control reaction lacking the enzyme is also shown and is important to define the magnitude of the observed burst.

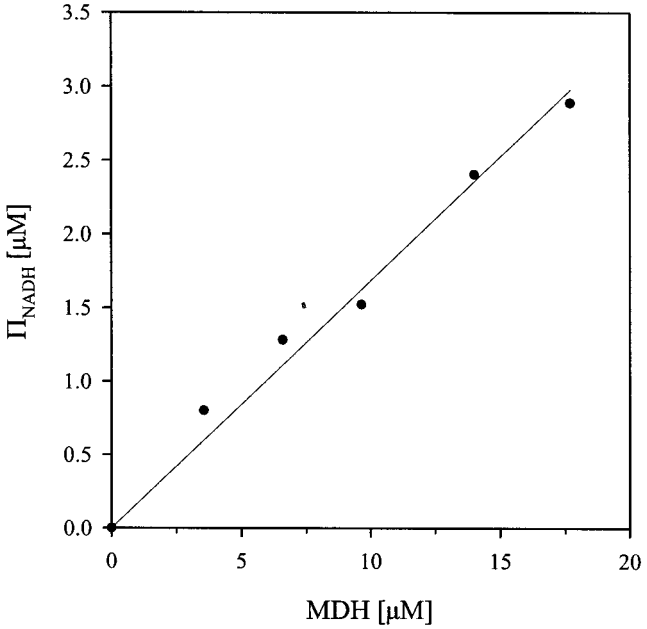

FIGURE 6: Burst diagram relating the molar concentration of NADH released in the pre-steady state (Π) to the total molar concentration of PsMDH active sites present. The solid line shows a straight line fit of the data that had been constrained to go through the origin. Reaction conditions are described under Materials and Methods. Because a significant part of the burst occurred in the dead time of the stopped-flow reaction analyzer, a well-defined initial absorbance value was required for the analysis (cf. Figure 5). The reported values for Π were confirmed in three independent experimental determinations and display standard deviations of approximately 15%. Π values estimated by the nonlinear fitting procedure (eq 9) and by graphical extrapolation were in close agreement (±7%). The concentration of PsMDH active sites is based on the molar extinction coefficient of the protein. Cofactor binding experiments, measured by fluorescence titration, indirectly confirmed the molar concentration of PsMDH active sites (±10%), assuming that the enzyme has a single binding site for NAD(H) (*14*).

(15 mM). The progress curves, recorded by the increase in $A_{340\ nm}$ due to reduction of NAD^+, displayed burst kinetics with an initial exponential increase in absorbance followed by a steady-state rate of NADH appearance, as shown in Figure 5. Comparison of representative stopped-flow traces measured in H_2O and in D_2O (Figure 5) did not reveal a sizable S-KIE on the transient rate. However, a normal S-KIE was found on the steady-state rate, approaching that seen in conventional initial-rate studies. The multiple-turnover progress curves for varied [PsMDH] were fitted to eq 9. Figure 6 shows the relationship between the estimated value of the burst (Π) and the molar concentration of PsMDH present. A straight-line fit of the data gave a slope value of 0.27 ($r^2 = 0.98$), indicating that ≈27% of the enzyme are turned over in the burst phase. In D_2O, the experimental Π values were similar to those seen in H_2O, the average ratio of $\Pi(H_2O)/\Pi(D_2O)$ being 0.92.

DISCUSSION

Steady-State Kinetic Mechanism at pH 10.0. Primary deuterium isotope effects on steady-state kinetic parameters for the foward and reverse reaction of MDH from *P. fluorescens* (eq 1) show that this enzyme catalyzes the oxidation of D-mannitol at the optimum pH of 10.0 by an ordered bi-bi mechanism in which NAD^+ binds before D-mannitol and D-fructose dissociates before NADH (Scheme 1; eq 10). The rate constants for the conversion of E-NADH into E + NADH (k_9) and, likewise, the conversion of E-NAD^+ into E + NAD^+ (k_2) have been calculated from kinetic constants in Table 1 as $k_9 = k_{catr}K_{iNADH}/K_{NADH} = 60\ s^{-1}$ and $k_2 = k_{cato}K_{iNAD+}/K_{NAD^+} = 129\ s^{-1}$ (*25*). Considering the turnover numbers in forward and reverse reaction at pH 10.0, the analysis suggests that k_9 is a major rate-limiting

Scheme 1: Kinetic Mechanism of PsMDH at pH 10.0 (eq 10), Where A Is NAD^+, B Is D-Mannitol, P Is D-Fructose, and Q Is NADH

$$E + A \underset{k_2}{\overset{k_1}{\rightleftharpoons}} EA + B \underset{k_4}{\overset{k_3}{\rightleftharpoons}} EAB \underset{k_6}{\overset{k_5}{\rightleftharpoons}} EPQ \underset{k_8}{\overset{k_7}{\rightleftharpoons}} EQ + P \underset{k_{10}}{\overset{k_9}{\rightleftharpoons}} E + Q$$

step for D-mannitol oxidation, whereas k_2 appears not to be rate-determining for D-fructose reduction. Partial rate limitation by steps involved in NADH release is supported by two other observations which require that there be a slow step after hydride transfer to NAD^+ as well as after release of D-fructose: (1) the detection of a significant primary deuterium isotope effect on $k_{cat}/K_{mannitol}$ but not on k_{cat} for the forward reaction; and (2) the detection of a pre-steady-state burst of formation of NADH in multiple turnover stopped-flow kinetic experiments for D-mannitol oxidation.

pL Profiles for NAD^+-Dependent Oxidation of D-Mannitol. The variation of $\log(k_{cat}/K_{mannitol})$ with pH reveals a single enzymic group in the E-NAD^+ complex with an apparent p*K* of 9.2, which must be unprotonated for substrate binding or catalysis. The pH profiles of $\log(k_{cat}/K_{fructose})$ (*14*) and $\log(k_{cat}/K_{mannitol})$ are mirror images one of another, as expected if they showed the pH-dependent ionization of the general acid−base catalyst of the reaction. The outward displacement by about 1.5 pH units in the pH profile of log k_{cato}, relative to the pH profile of $\log(k_{cat}/K_{mannitol})$, appears to be a

Scheme 2: Expanded pH-Dependent Mechanism of PsMDH Catalysis (eq 11)[a]

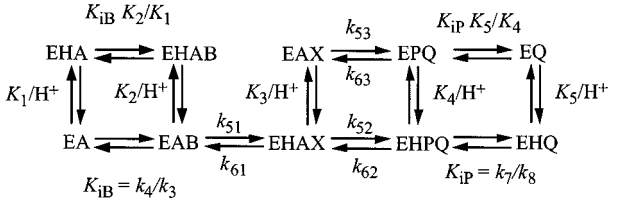

[a] Binding of B and P are assumed to be in rapid equilibrium, and rate constant numbering builds on eq 10.

manifestation of both partly rate-limiting release of NADH and perturbations in pK brought about upon formation of the ternary complex. The pD profiles for $\log(k_{cat}/K_{mannitol})$ and $\log k_{cato}$ display identical pK shifts of about +0.4 pH units relative to the pH profiles of the corresponding kinetic parameters. The magnitude of the observed ΔpK ($=pK_D - pK_H$) is quite common for the ionization of acidic groups in proteins and probably reflects mainly the fractionation factor for H_3O^+, $\Phi(H_3O^+) \approx 0.33$ (*23*).

KIEs and Their pH Dependences.[4] Slatner et al. (*14*) have shown that $^D(k_{cat}/K_{fructose})$ for PsMDH decreases above a pK of 9.3 where the pH-dependent step of the reaction becomes completely rate-limiting, indicating that hydride transfer from NADH is not pH-dependent. The limiting value of $^D(k_{cat}/K_{fructose})$ at high pH was not clear in the previous study of PsMDH; therefore, it remained elusive whether the hydride transfer occurs before or after the auxiliary pH-dependent step (*14*). Here, careful measurements of $^D(k_{cat}/K_{fructose})$ at pH values above the pK of 9.3 yielded a value of 0.83 which is close to the reported value of 0.85 for the equilibrium isotope effect on NADH-dependent carbonyl group reduction (*28*).[5] Hence, the pH-dependent step in the mechanism of PsMDH occurs after the hydride transfer step. Now, if the apparent pK of 9.3 in the pH profiles of k_{cat}/K truly represents the pH-dependent ionization of the general acid−base catalyst of the reaction, the variation KIE on $k_{cat}/K_{fructose}$ with pH requires a stepwise mechanism of chemical carbonyl group reduction by PsMDH. In this mechanism, hydride transfer to carbon precedes proton transfer to oxygen and an alkoxide intermediate is formed that cannot dissociate from the enzyme until it has become protonated by an enzyme catalytic group (eq 11; Scheme 2). In an alternative scenario, there may be an internal equilibrium after C−H and O−H bond formation that involves the D-mannitol-bound enzyme and is sensitive to solution conditions, thus pH. In that case, the observed pK value of ≈9.3 would reflect the ionization of an enzyme group that determines the post-catalytic equilibrium (for the reverse reaction). We cannot distinguish clearly between the two possibilities but discuss the results in the frame of eq 11 which is a chemically reasonable mechanism that does not need to invoke a pH-dependent conformational equilibrium at the ternary complex level.

The isotope effect on $k_{cat}/K_{mannitol}$ decreases from 1.9 at pH 9.0 to 1.1 at pH 10.5. This variation of $^D(k_{cat}/K_{mannitol})$ with pH is as predicted by eq 11. The limiting value for $^D(k_{cat}/K_{mannitol})$ is likely 1.0, which reflects the large forward commitment of the E-NAD$^+$−alkoxide complex to undergo hydride transfer when, at high pH, the ratio of E-NAD$^+$−alkoxide to EH-NAD$^+$−alkoxide approaches a zero value.

At low pH (≤9), PsMDH displays a pH-independent and sizable KIE on $k_{cat}/K_{mannitol}$, suggesting that D-mannitol is not sticky at the pH optimum. The significant KIE on $k_{cat}/K_{mannitol}$ (≈1.8) implies a forward commitment, $C_f = k_{52}/k_{61}$, which cannot be very large. If we assume a value of ≈6.5 for the intrinsic isotope effect of hydride transfer by alcohol dehydrogenases (*29*), k_{52}/k_{61} should have a value of ≈6. In reverse reaction at low pH, a reverse commitment of k_{52}/k_{61} is expected; therefore, $^D(k_{cat}/K_{mannitol})/^DK_{eq}$ should equal $^D(k_{cat}/K_{fructose})$, and a reasonable agreement between the measured value of 2.4−2.5 (*14*) and a calculated value of 2.29 (=1.9/0.83) values was found. Because $1 + k_{61}/k_{52}$ equals 1.17, and its log is < 0.1, the effect of k_{52}/k_{61} on the pH profiles of $k_{cat}/K_{mannitol}$ and $k_{cat}/K_{fructose}$, described by the expressions (*15*, *16*) $pK_{app} = pK_1 - \log(1+ k_{61}/k_{52})$ and $pK_{app} = pK_1 + \log(1+ k_{61}/k_{52})$, respectively, should be hardly noticed. This agrees well with the experimental findings. Therefore, the pK of the group responsible for the decrease of the k_{cat}/K profiles can be assigned with reasonable certainty as 9.2−9.3 in both E-NAD$^+$ and E-NADH. If we assume that $pK_1 = 9.3 \approx pK_3$ and $k_{52}/k_{61} \approx 6$, the expression $pK_{app} = pK_3 + \log[(k_{61}+k_{52})/k_{53}]$ (*15*) and the observed pK for the $^D(k_{cat}/K)$ profiles of 9.6 (*14*) can be used to obtain an estimate of for k_{52}/k_{53} of 2.3. The analysis shows that deprotonation of EH-NAD$^+$-D-mannitol does not lead to a substantial slowing of the hydride transfer step.

The variations of $^Dk_{cat}$ and $^D(k_{cat}/K_{mannitol})$ with pH in the pH range 6.0−9.0 are interesting. The KIE on k_{cat} shows a plateau around pH 8 with an average value of 1.07, indicating that product release steps are mainly but not completely rate-limiting in this pH range. At pH ≤ 7.7, $^Dk_{cat}$ increases to a constant value of 1.21, which is smaller than $^D(k_{cat}/K_{mannitol})$. Mechanism 11 implies that KIEs on k_{cat} and $k_{cat}/K_{mannitol}$ approach the same limiting value at low pH, at variance with the experimental observations. The results require that some step, occurring either after D-fructose has dissociated or before D-mannitol has bound, be partly rate-limiting for k_{cat} and decrease as the pH is decreased so that the ratio of it and the chemical reaction remains constant.

Solvent Isotope Effects, Multiple Isotope Effects, and Proton Inventories. The sizable S-KIE on $k_{cat}/K_{mannitol}$ and the (linear) proton inventory plot for the same kinetic parameter suggest that a single catalytic proton bridge contributes to stabilization of the transition state of D-mannitol oxidation by PsMDH.[6] Considering the relationship $^{D_2O}(k_{cat}/K_{mannitol}) = \Phi^{RS}/\Phi^{TS}$ and assuming a value of 1 for the reactant state fractionation factor Φ^{RS}, the observed value of 2.36 for the S-KIE on $k_{cat}/K_{mannitol}$ implies a transition-state fractionation factor of 0.42.[7,8] In the direction of

[4] Because there is only one isotope-sensitive step in the PsMDH-catalyzed reaction (eq 10), the following equations provide the basic framework for the analysis of KIEs on steady-state kinetic parameters: $^D(k_{cat}/K) = (^Dk_5 + C_f + {}^DK_{eq}C_r)/(1 + C_f + C_r)$ and $^Dk_{cat} = (^Dk_5 + C_{Vf} + {}^DK_{eq}C_r)/(1 + C_{Vf} + C_r)$, where $^Dk_5$ is the isotope effect of k_5 (eq 10), and C_f and C_r are commitment factors (*26*, *27*) in the forward and reverse reaction, respectively. $^DK_{eq}$ is the equilibrium isotope effect, and C_{Vf} is a comparison between the rate constant of the isotope-sensitive step and all other forward unimolecular steps (*26*, *27*).

[5] The normal KIE on $k_{cat}/K_{fructose}$ seen in D_2O at pD 10.0 may reflect an outward displacement of the pL profile of $^D(k_{cat}/K_{fructose})_{D_2O}$, relative to that of $^D(k_{cat}/K_{fructose})_{H_2O}$.

[6] We stress that the one-proton model provides the simplest interpretation of the proton inventory plot for $k_{cat}/K_{mannitol}$. The precision level of $k_{cat}/K_{mannitol}$ was, however, above the theoretical threshold for the statistical discrimination among linear and polynomical models (*23*).

D-mannitol oxidation (eq 11), the step represented by k_{51} is the only one that should display a solvent isotope effect. At pH 10.0, however, conversion of EH-NAD^+−alkoxide into E-NAD^+−alkoxide is quasi-irreversible, and k_{51} is most likely faster than k_{53}. Therefore, this suggests that a step other than k_{51} is responsible for the observed S-KIE on $k_{cat}/K_{mannitol}$. The equivalence of $^{D}(k_{cat}/K_{mannitol})$ in H_2O and D_2O indicates that the enzymic hydride transfer to NAD^+ takes place in a concerted fashion[9] with another partly rate-limiting proton-transfer process that could be part of a proton relay. In other words, the S-KIE is on k_{53}.

The magnitude of S-KIE on k_{cat}, relative to $^{D_2O}(k_{cat}/K_{mannitol})$, suggests that a step outside the catalytic sequence represented by $k_{cat}/K_{mannitol}$ occurs at a slower rate in D_2O than in H_2O. The observation of an S-KIE on the steady-state rate, but not on the transient rate in multiple-turnover stopped-flow reactions at saturating D-mannitol levels, agrees well with the contention that $^{D_2O}k_{cat}$ reflects mainly $^{D_2O}k_9$. A normal value of $\approx$2 for $^{D_2O}k_9$ explains quantitatively the observed 2-fold tighter binding of NADH in D_2O than in H_2O. The proton inventory for k_{cat} suggests that a single solvation proton bridge contributes to the observed isotope effect.

In summary, this paper describes a stepwise reaction mechanism of NAD^+-dependent secondary alcohol oxidation by PsMDH in which a pH-dependent internal equilibrium involving D-mannitol-bound enzyme precedes the rate-limiting C−H bond cleavage. Proton removal from the reactive 2-OH may take place in this pre-equilibrium. Loss of a proton (probably as H_2O rather than H_3O^+) at high pH either from the acid/base catalyst if the alkoxide mechanism is operable or from another auxiliary enzyme group that determines the precatalytic isomerization step leads to trapping of a reaction intermediate that shows a very high commitment to undergo hydride transfer to give D-fructose. A proton is in flight in the transition state of C−H bond cleavage. The alkoxide mechanism would imply that PsMDH, which unlike medium-chain ADH (*15*−*20*, *31*) does not contain catalytic Zn^{2+}, must utilize enzyme-mediated electrophilic interactions to facilitate proton removal from the reactive alcohol group before the C−H bond is broken.

ACKNOWLEDGMENT

The authors thank Gerhard Mayer for the preparation of deuterated D-mannitol and Dr. Michael Puchberger for NMR measurements. Professor C. Obinger (Institute of Chemistry, University of Agricultural Sciences Vienna) kindly provided access to the stopped-flow instrument in his laboratory. The expert and patient assistance of Dr. P.-G. Furtmüller in acquiring transient kinetic data is gratefully acknowledged.

REFERENCES

1. Hummel, W., and Kula, R. (1989) *Eur. J. Biochem. 184*, 1−13.
2. Liese, A., Karutz, M., Kamphuis, J., Wandrey, C., and Kragl, U. (1996) *Biotechnol. Bioeng. 51*, 544−550.
3. Jörnvall, H., Persson, B., Krook, M., Atrian, S., Gonzalez-Duarte, R., Jeffery, J., and Ghosh, D. (1995) *Biochemistry 34*, 6003−6013.
4. Persson, B., Zigler, S., Jr., and Jörnvall, H. (1994) *Eur. J. Biochem. 226*, 15−22.
5. Persson, B., Jeffery, J., and Jörnvall, H. (1991) *Biochem. Biophys. Res. Commun. 177*, 218−223.
6. Benach, J., Atrian, R., Gonzalez-Duarte, R., and Ladenstein, R. (1998) *J. Mol. Biol. 282*, 383−399.
7. Benach, J., Atrian, R., Gonzalez-Duarte, R., and Ladenstein, R. (1999) *J. Mol. Biol. 289*, 335−355.
8. Eklund, H., Horjales, E., Jörnvall, H., Bränden, C.-I., and Jeffery, J. (1985) *Biochemistry 24*, 8005−8012.
9. Johansson, K., E.-Ahmad, M., Kaiser, C., Jörnvall, H., Eklund, H., Höög, J.-O., and Ramaswamy, S. (2001) *Chem.-Biol. Interact. 130*−*132*, 351−358.
10. Ruzheinikov, S. N., Burke, J., Sedelnikova, S., Baker, P. J., Taylor, R., Bullough, P. J., Muir, N. M., Gore, M. G., and Rice, D. W. (2001) *Structure 9*, 789−802.
11. Klinman, J. P. (1981) *CRC Crit. Rev. Biochem. 10*, 39−78.
12. Schneider, K.-H., Giffhorn, F., and Kaplan, S. (1993) *J. Gen. Microbiol. 139*, 2475−2484.
13. Brunker, P., Altenbuchner, J., Kulbe, K. D., Mattes, R (1998) *Biochim. Biophys. Acta 1351*, 157−167.
14. Slatner, M., Nidetzky, B., Kulbe, K. D. (1999) *Biochemistry 38*, 10489−10498.
15. Cook, P. F., and Cleland, W. W. (1981) *Biochemistry 20*, 1805−1816.
16. Cook, P. F. (1991) in *Enzyme Mechanism From Isotope Effects* (Cook, P. F., Ed.) pp 203−245, CRC Press, Boca Raton, FL.
17. Pettersson, G. (1987) *CRC Crit. Rev. Biochem. 21*, 349−389.
18. Ohno, A., and Ushio, K. (1986) in *Coenzymes and Cofactors* (Dolphin, D., Poulson, R., and Avramovic, O., Eds.) Vol. II, Part B, pp 275−332, John Wiley and Sons, New York.
19. Luo, J., and Bruice, T. C. (2001) *J. Am. Chem. Soc. 123*, 11952−11959.
20. Sekhar, V. C., and Plapp, B. V. (1990) *Biochemistry 29*, 4289−4295.
21. Deng, H., Schindler, J. F., Berst, K. B., Plapp, B., and Callender, R. (1998) *Biochemistry 37*, 14267−14278.
22. Mostad, S. B., and Glasfeld, A. (1993) *J. Chem. Educ. 70*, 504−506.
23. Schowen, K. B., and Schowen, R. L. (1982) *Methods Enzymol. 87*, 551−606.
24. Northrop, D. B. (1982) *Methods Enzymol. 87*, 607−625.
25. Segel, I. (1993) *Enzyme Kinetics*, Wiley Classics Library Edition, pp 588−589, Wiley-Interscience, New York.
26. Cleland, W. W. (1990) in *The Enzymes* (Boyer, P. D., and Krebs, E. G., Eds.) 3rd. ed., pp 99−158, Academic Press, San Diego, CA.
27. Cook, P. F., and Cleland W. W. (1981) *Biochemistry 20*, 1790−1796.
28. Cook, P. F., Blanchard, J. S., and Cleland, W. W. (1980) *Biochemistry 19*, 4853−4858.
29. Scharschmidt, M., Fischer, M. A., and Cleland, W. W. (1984) *Biochemistry 23*, 5471−5478.
30. Cleland, W. W. (1991) in *Enzyme Mechanism From Isotope Effects* (Cook, P. F., Ed.) pp 247−265, CRC Press, Boca Raton, FL.
31. Ramaswamy, S., Park, D.-H., and Plapp, B. V. (1999) *Biochemistry 38*, 13951−13959.

BI025517X

[7] Incubation of the E−NAD^+ complex with Ellman's reagent did not reveal the presence of a fast-reacting essential thiol group that might have caused a Φ^{RS} value different from unity. After extended reaction times of up to 1 h, a number of 6−7 accessible cysteins per each native PsMDH molecule was counted by colorimetric titration.

[8] The solvent isotope effect on $k_{cat}/K_{fructose}$ at pH 10.0 was inverse. Values of 0.30 ± 0.04 and 0.66 ± 0.11 were measured with NADH and NADD as the coenzyme, respectively. Note, however, that the observed S-KIE on $k_{cat}/K_{fructose}$ includes a solvent effect on p*K*.

[9] The multiple deuterium isotope effect method (*30*) was used to probe the stepwise mechanism of hydride transfer and proton transfer in the PsMDH-catalyzed oxidation of D-mannitol. If the chemical reaction was concerted, hydride and proton transfer would be independent of one another; thus, equivalence of substrate isotope effects in H_2O and D_2O would be expected.